Advances in Nano Research, *Vol. 4, No. 4 (2016) 309-326*
DOI: http://dx.doi.org/10.12989/anr.2016.4.4.309

Buckling of a single-layered graphene sheet embedded in visco-Pasternak's medium via nonlocal first-order theory

Ashraf M. Zenkour*[1,2]

[1]*Department of Mathematics, Faculty of Science, King Abdulaziz University, Jeddah 21589, Saudi Arabia*
[2]*Department of Mathematics, Faculty of Science, Kafrelsheikh University, Kafrelsheikh 33516, Egypt*

(Received March 17, 2016, Revised June 16, 2016, Accepted November 7, 2016)

Abstract. The buckling response of a single-layered graphene sheet (SLGS) embedded in visco-Pasternak's medium is presented. The nonlocal first-order shear deformation elasticity theory is used for this purpose. The visco-Pasternak's medium is considered by adding the damping effect to the usual foundation model which characterized by the linear Winkler's modulus and Pasternak's (shear) foundation modulus. The SLGS be subjected to distributive compressive in-plane edge forces per unit length. The governing equilibrium equations are obtained and solved for getting the critical buckling loads of simply-supported SLGSs. The effects of many parameters like nonlocal parameter, aspect ratio, Winkler-Pasternak's foundation, damping coefficient, and mode numbers on the buckling analysis of the SLGSs are investigated in detail. The present results are compared with the corresponding available in the literature. Additional results are tabulated and plotted for sensing the effect of all used parameters and to investigate the visco-Pasternak's parameters for future comparisons.

Keywords: nonuniform buckling; nonlocal shear deformation model; visco-Pasternak's medium

1. Introduction

Ever since the graphene was discovered by Geim and Novoselov (Novoselov, Geim *et al.* 2004), many investigations have been published in the literature about vibration, buckling and wave propagation of nano graphene sheets. Graphene is a monolayer arranged in a honeycomb lattice with a unique series of unprecedented structural, mechanical and electrical properties (Basua and Bhattacharyya 2012). Nano structural elements include nanotubes, nanobeams, nanoplates, nanosheets and nanocones. Nano structure components have widely applications in micro/nano electromechanical systems (MEMS/NEMS), nano sensors, electrical batteries, biomedical, bioelectrical, reinforcement role at composites, etc. (Lim, Li *et al.* 2010, Ghorbanpour Arani, Amir *et al.* 2014, Sakhaee-Pour, Ahmadian *et al.* 2008, Wang, Li *et al.* 2012, Li, Li *et al.* 2011, Pantelic, Meyer *et al.* 2012). Due to its potential, nano graphene sheets are used in nano technology, particularly in recent years utilized in buckling of graphene sheets with/without conveying viscosity.

In order to study the mechanical behavior of nanostructures, it has been reported that the small

*Corresponding author, Professor, E-mail: zenkour@kau.edu.sa, zenkour@sci.kfs.edu.eg

http://www.techno-press.com/?journal=anr&subpage=7 ISSN: 2287-237X (Print), 2287-2388 (Online)

scale effect must play an important role in the nanoscale structures, but this small scale effect has been ignored when classical local continuum theory was adopted (Xu, Shen *et al.* 2013). In recent years, various size-dependent continuum theories such as couple stress theory (Reddy 2011), strain gradient elasticity theory (Akgöz and Civalek 2013a, b, Lam, Yang *et al.* 2003), modified couple stress theory (Ke, Wang *et al.* 2012, Akgöz and Civalek 2011, Akgö and Civalek 2013c, Yang, Chong *et al.* 2002, Akgöz and Civalek 2012) and nonlocal elasticity theory (Eringen and Edelen 1972, Eringen 1983, 2002, 2006) are proposed. These theories are comprised of information about the interatomic forces and internal lengths that is introduced as small scale effect in nonlocal elasticity theory (Eringen 2006).

In this regard, Pradhan and Murmu (2009) have studied the small scale effect on the buckling analysis of biaxially compressed single-layered graphene sheets (SLGSs) using nonlocal continuum mechanics. Sakhaee-Pour (2009) has investigated the elastic buckling behavior of defect-free SLGS using an atomistic modeling approach. Farajpour, Solghar *et al.* (2013a) have investigated the nonlinear buckling characteristics of MLGSs subjected to non-uniformly distributed in-plane load through the thickness. Farajpour, Solghar *et al.* (2013b) have studied the axisymmetric buckling analysis of circular SLGSs by decoupling the basic constitutive equations based on the nonlocal theory of Eringen. Ansari and Sahmani (2013) have studied the biaxial buckling behavior of SLGSs. They have incorporated Eringen's nonlocal elasticity equations into different plate theories to consider the size-effects in the analysis. Mohammadi, Farajpour *et al.* (2014) have studied the buckling behavior of orthotropic rectangular nanoplate. They have implemented the nonlocal elasticity theory to investigate the shear buckling of orthotropic SLGSs in thermal environment.

Literature shows that research on SLGSs or MLGSs embedded in elastic medium are becoming increasing common for more accurate design and analysis of micro and nanostructures. Pradhan and Murmu (2010) have investigated the buckling behavior of SLGS embedded in an elastic medium by implementing the nonlocal elasticity theory based on the classical plate theory. Samaei, Abbasion *et al.* (2011) have discussed the effect of length scale on buckling behavior of a SLGS embedded in a Pasternak elastic medium using the nonlocal Mindlin plate theory. Radić, Jeremić *et al.* (2014) have presented the buckling of double-orthotropic nanoplates based on nonlocal elasticity theory. They have assumed that two nanoplates are bonded by an internal elastic medium and surrounded by external elastic foundation. Anjomshoa, Shahidi *et al.* (2104) have developed a finite element approach based on the size dependent nonlocal elasticity theory for buckling analysis of nano-scaled MLGSs embedded in polymer matrix. Golmakani and Rezatalab (2015) have investigated the non-uniform biaxial buckling analysis of orthotropic SLGS embedded in a Pasternak elastic medium. They have used the nonlocal Mindlin plate theory to derive the nanoplate equilibrium equations in terms of generalized displacements. Karličić, Cajić *et al.* (2015) have presented the thermal vibration and stability analysis of the multi-layered graphene sheets (MLGSs) modeled as multi-nanoplate system (MNPS) embedded in an elastic medium. They used the nonlocal Kirchhoff-Love plate theory to derive the governing equations and to obtain their exact closed-form solutions for nonlocal frequencies, critical buckling loads and critical buckling temperature by using the Navier's and trigonometric methods. Zhang, Zhang *et al.* (2016) have presented the critical buckling loads of SLGSs by solving the governing differential equations derived from the principle of minimum potential energy using the element-free kp-Ritz method.

In spite of many researches about buckling responses of SLGSs using nonlocal elasticity theory, there are limited studies that consider nonlocal visco-elastic systems. However, to date, no

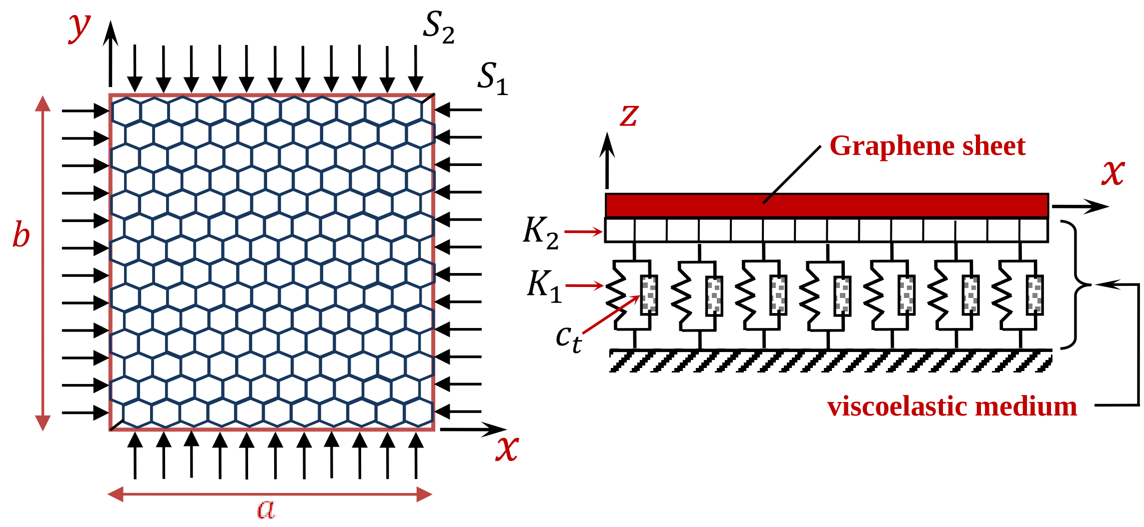

Fig. 1 A continuum plate model of a single-layered graphene sheet embedded in a viscoelastic medium

report has been found in the literature on the nonuniform buckling analyses of graphene sheets embedded in visco-elastic medium via a nonlocal theory. Motivated by these considerations, in order to improve design of nano coupled system we aim to study the buckling analysis of visco-SLGSs system based on the first-order shear deformation theory. SLGSs are conveying viscous fluid and coupled by visco-Pasternak's medium. The closed-form solutions are obtained to indicate the characteristic parameters of coupled visco-SLGSs. The results of this study is hoped to be use to design this kind of nano devices.

2. Basic equations of single-layered graphene sheet (SLGS)

Let us consider a single-layered graphene sheet (SLGS) of length a, width b and uniform thickness h as shown in Fig. 1. The SLGS is made of a homogeneous isotropic and linearly elastic material with Young's modulus E, Poisson's ratio ν, shear modulus $G = E/2(1+\nu)$ and material density ρ. Suppose that the upper surface of the SLGS $(z = h/2)$ be subjected to a transverse distribution mechanical load $q(x, y)$. In addition, there are distributive compressive in-plane edge forces S_1 and S_2 per unit length (applied in the directions x and y, respectively, and considered positive in tension).

2.1 Nonlocal first-order plate theory

The most general form of the constitutive relation in nonlocal elasticity theory involves an integral over the entire region of interest. The integral contains a nonlocal kernel function, which describes the relative influence of the strains at various locations of the body on the stress at the material point under consideration. Specifically, the constitutive equations of nonlocal elasticity for homogenous and isotropic elastic solids read

$$\sigma_{kl}(x) = \int_V \vartheta(|x - x'|)\tau_{kl}(x')\mathrm{d}V(x'), \tag{1}$$

where σ_{ij} is the nonlocal stress tensor, V is the volume occupied by the elastic body, $|x - x'|$ denotes distance in Euclidean space, and the nonlocal kernel $\vartheta(|x - x'|)$ accounts for the effect of the strain at the point x' on the stress at the point x in the elastic body.

The quantities $\tau_{kl}(x')$ denote the components of local stress tensor for which the standard local constitutive equations are adopted, i.e.

$$\tau_{kl}(x') = \frac{E}{1+\nu}\left[\varepsilon_{kl}(x') + \frac{\nu}{1-\nu}\varepsilon_{mm}(x')\delta_{kl}\right], \tag{2}$$

where $\varepsilon_{kl}(x')$ are the components of classical local strain tensor at x'. The dynamic equations and small strain-displacement relations for a linear homogenous elastic body using nonlocal elasticity theory are given by the usual relations

$$\sigma_{kl,l} + f_k = \rho\frac{\partial^2 u_k}{\partial t^2}, \quad \varepsilon_{kl}(x') = \frac{1}{2}\left[\frac{\partial u_k(x')}{\partial x'_l} + \frac{\partial u_l(x')}{\partial x'_k}\right], \quad \gamma_{kl} = 2\varepsilon_{kl}, \tag{3}$$

where $u_k(x')$ are the components of displacement vector at the reference point x' in the body and f_k are the body forces. For an appropriate form of the nonlocal kernel (Eringen and Edelen 1972, Eringen 1983, 2002, 2006), it turns out that the nonlocal internal constitutive relation given by Eq. (1) can be inverted to yield the following pseudo-local constitutive equation of gradient type

$$[1 - (le_0)^2\nabla^2]\sigma_{kl} = \tau_{kl}. \tag{4}$$

The parameter l is an internal characteristic length (e.g., lattice parameter, granular distance), and e_0 is a material constant determined by experiment or by matching dispersion curves of plane waves with those of atomic lattice dynamics. One may see that when the internal characteristic length l is neglected, i.e., the particles of the medium are considered to be continuously distributed and interacting without long-range forces, le_0 is zero, and Eq. (4) reduces to the constitutive equations of classical local elasticity theory.

The first-order shear deformation theory is used for the present SLGS. The displacement field can be written as

$$\begin{aligned} u_1(x,y,z) &= u(x,y) + z\,\psi(x,y), \\ u_2(x,y,z) &= v(x,y) + z\,\varphi(x,y), \\ u_3(x,y,z) &= w(x,y), \end{aligned} \tag{5}$$

where u_1, u_2, and u_3 are the displacements in the x, y, and z directions, u, v, and w are the mid-plane displacements. Here u and v are the in-plane displacements while w is the transverse displacement (deflection), and ψ and φ are the rotational displacement about y and x axes, respectively. The displacements of the classical plate theory are given by setting $\psi = -\frac{\partial w}{\partial x}$ and $\varphi = -\frac{\partial w}{\partial y}$.

By substituting the displacement relations given in Eq. (5) into the strain-displacement equations of elasticity, the normal and shear strain components are obtained as

$$\begin{Bmatrix}\varepsilon_{xx}\\ \varepsilon_{yy}\\ \gamma_{xy}\end{Bmatrix} = \begin{Bmatrix}\dfrac{\partial u}{\partial x}\\ \dfrac{\partial v}{\partial y}\\ \dfrac{\partial v}{\partial x} + \dfrac{\partial u}{\partial y}\end{Bmatrix} + z\begin{Bmatrix}\dfrac{\partial \psi}{\partial x}\\ \dfrac{\partial \varphi}{\partial y}\\ \dfrac{\partial \varphi}{\partial x} + \dfrac{\partial \psi}{\partial y}\end{Bmatrix}, \quad \varepsilon_{zz} = 0, \quad \begin{Bmatrix}\gamma_{yz}\\ \gamma_{xz}\end{Bmatrix} = \begin{Bmatrix}\varphi + \dfrac{\partial w}{\partial y}\\ \psi + \dfrac{\partial w}{\partial x}\end{Bmatrix}. \tag{6}$$

The corresponding stress-strain relationships, accounting for the thermal effects, in the isotropic SLGS coordinates can be expressed as

$$\begin{Bmatrix} \sigma_{xx} - \xi \nabla^2 \sigma_{xx} \\ \sigma_{yy} - \xi \nabla^2 \sigma_{yy} \end{Bmatrix} = \frac{E}{1-\nu^2} \begin{bmatrix} 1 & \nu \\ \nu & 1 \end{bmatrix} \begin{Bmatrix} \varepsilon_{xx} \\ \varepsilon_{yy} \end{Bmatrix}, \quad \begin{Bmatrix} \sigma_{yz} - \xi \nabla^2 \sigma_{yz} \\ \sigma_{xz} - \xi \nabla^2 \sigma_{xz} \\ \sigma_{xy} - \xi \nabla^2 \sigma_{xy} \end{Bmatrix} = G \begin{Bmatrix} \gamma_{yz} \\ \gamma_{xz} \\ \gamma_{xy} \end{Bmatrix}, \tag{7}$$

where $\xi = (le_0)^2$ represents the nonlocal parameter.

2.2 The visco-Winkler-Pasternak foundations

The two-parameter Pasternak's model is the most natural extension to the one-parameter Winkler's model. It considers a shear interaction between the spring elements by connecting the ends of the springs to a plate of an incompressible shear layer. The present SLGS is embedded in a homogeneous three-parameter viscoelastic medium. The foundation model is characterized by the linear Winkler's modulus K_1, the Pasternak's (shear) foundation modulus K_2, and the damping coefficient c_t of the viscoelastic medium. Taking into account the un-bonded contact between the SLGS and medium, the interaction follows the three-parameter visco-Pasternak's-type foundation model as (Zenkour 2016 a, b)

$$R_f = \left(K_1 - K_2 \nabla^2 + c_t \frac{\partial}{\partial t}\right) w, \tag{8}$$

where w is the transverse displacement and ∇^2 is the Laplacian (second-order spatial gradient). If the foundation is modelled as the visco-Winkler foundation, the coefficient K_2 in Eq. (1) is zero. The viscosity term may be omitted by setting $c_t = 0$ to get the analysis of the SLGS embedded in pure elastic medium.

2.3 Governing equations

The governing equations of motion can be obtained by using the principle of virtual displacements which yields

$$\int_{-h/2}^{h/2} \int_{\Omega} \left(\sigma_{xx} \delta\varepsilon_{xx} + \sigma_{yy} \delta\varepsilon_{yy} + \sigma_{xy} \delta\gamma_{xy} + \sigma_{xz} \delta\gamma_{xz} + \sigma_{yz} \delta\gamma_{yz}\right) \mathrm{d}\Omega \, \mathrm{d}z$$
$$- \int_{\Omega} \left(q - S_1 \frac{\partial w}{\partial x} \frac{\partial}{\partial x} - S_2 \frac{\partial w}{\partial y} \frac{\partial}{\partial y} - R_f\right) \delta w \, \mathrm{d}\Omega = 0. \tag{9}$$

So, the governing equations can be derived from the above functional by integrating the displacement gradients in ε_{ij} by parts. The extremum conditions of the obtained functional gives the following equilibrium equations

$$\begin{gathered} \frac{\partial N_{xx}}{\partial x} + \frac{\partial N_{xy}}{\partial y} = 0, \quad \frac{\partial N_{xy}}{\partial x} + \frac{\partial N_{yy}}{\partial y} = 0, \\ \frac{\partial Q_x}{\partial x} + \frac{\partial Q_y}{\partial y} + q - R_f + \frac{\partial}{\partial x}\left(S_1 \frac{\partial w}{\partial x}\right) + \frac{\partial}{\partial y}\left(S_2 \frac{\partial w}{\partial y}\right) = 0, \\ \frac{\partial M_{xx}}{\partial x} + \frac{\partial M_{xy}}{\partial y} - Q_x = 0, \quad \frac{\partial M_{xy}}{\partial x} + \frac{\partial M_{yy}}{\partial y} - Q_y = 0, \end{gathered} \tag{10}$$

where N_{xx}, N_{xy}, and N_{yy} are the basic components of stress resultants; M_{xx}, M_{xy}, and M_{yy} are the basic components of stress couples; and Q_x and Q_y are the shear stress resultants. They can be obtained by integrating Eq. (7) over the thickness of the plate as

$$\begin{gathered}
\{N_{xx}, N_{yy}, N_{xy}\} = \int_{-h/2}^{h/2} \{\sigma_{xx}, \sigma_{yy}, \sigma_{xy}\}\mathrm{d}z\,, \\
\{M_{xx}, M_{yy}, M_{xy}\} = \int_{-h/2}^{h/2} z\{\sigma_{xx}, \sigma_{yy}, \sigma_{xy}\}\mathrm{d}z\,, \\
\{Q_x, Q_y\} = k\int_{-h/2}^{h/2} \{\sigma_{xz}, \sigma_{yz}\}\mathrm{d}z\,,
\end{gathered} \tag{11}$$

where k is the transverse shear correction factor. Using the stress-strain relationships, Eq. (7), and the stress resultants definition, Eq. (11), with the aid of Cauchy's relations, Eq. (6), we can express the stress resultants in terms of the displacements as follows

$$\begin{Bmatrix} N_{xx} - \xi\nabla^2 N_{xx} \\ N_{yy} - \xi\nabla^2 N_{yy} \\ N_{xy} - \xi\nabla^2 N_{xy} \end{Bmatrix} = \frac{Eh}{1-\nu^2}\begin{bmatrix} 1 & \nu & 0 \\ \nu & 1 & 0 \\ 0 & 0 & \frac{1-\nu}{2} \end{bmatrix}\begin{Bmatrix} \frac{\partial u}{\partial x} \\ \frac{\partial v}{\partial y} \\ \frac{\partial v}{\partial x} + \frac{\partial u}{\partial y} \end{Bmatrix}, \tag{12a}$$

$$\begin{Bmatrix} M_{xx} - \xi\nabla^2 M_{xx} \\ M_{yy} - \xi\nabla^2 M_{yy} \\ M_{xy} - \xi\nabla^2 M_{xy} \end{Bmatrix} = D\begin{bmatrix} 1 & \nu & 0 \\ \nu & 1 & 0 \\ 0 & 0 & \frac{1-\nu}{2} \end{bmatrix}\begin{Bmatrix} \frac{\partial \psi}{\partial x} \\ \frac{\partial \varphi}{\partial y} \\ \frac{\partial \varphi}{\partial x} + \frac{\partial \psi}{\partial y} \end{Bmatrix}, \tag{12b}$$

$$\begin{Bmatrix} Q_y - \xi\nabla^2 Q_y \\ Q_x - \xi\nabla^2 Q_x \end{Bmatrix} = kGh\begin{Bmatrix} \varphi + \frac{\partial w}{\partial y} \\ \psi + \frac{\partial w}{\partial x} \end{Bmatrix}, \tag{12c}$$

where $D = \frac{Eh^3}{12(1-\nu^2)}$ is the bending rigidity of the SLGS.

The substitution of Eqs. (12) into Eqs. (10) gives the following nonlocal governing partial differential equations in terms of displacements w, ψ, and φ only

$$\kappa Gh\left(\frac{\partial\psi}{\partial x} + \frac{\partial\varphi}{\partial y} + \nabla^2 w\right) - (1 - \xi\nabla^2)P = 0, \tag{13a}$$

$$D\left(\frac{\partial^2\psi}{\partial x^2} + \frac{1+\nu}{2}\frac{\partial^2\varphi}{\partial x\partial y} + \frac{1-\nu}{2}\frac{\partial^2\psi}{\partial y^2}\right) - kGh\left(\psi + \frac{\partial w}{\partial x}\right) = 0, \tag{13b}$$

$$D\left(\frac{1-\nu}{2}\frac{\partial^2\varphi}{\partial x^2} + \frac{1+\nu}{2}\frac{\partial^2\psi}{\partial x\partial y} + \frac{\partial^2\varphi}{\partial y^2}\right) - kGh\left(\varphi + \frac{\partial w}{\partial y}\right) = 0, \tag{13c}$$

where

$$P(x,y) = \left(K_1 - K_2\nabla^2 + C_t\frac{\partial}{\partial t}\right)w - \frac{\partial}{\partial x}\left(S_1\frac{\partial w}{\partial x}\right) - \frac{\partial}{\partial y}\left(S_2\frac{\partial w}{\partial y}\right). \tag{14}$$

3. Solution of nonlocal static buckling response

The determination of critical buckling loads is of fundamental importance in the design of many nano-structures. The buckling formulation begins by assuming a solution of the displacement field and the thermal field. For the simply-supported SLGS we have the following boundary conditions

$$\begin{aligned} w = \varphi = M_{xx} = 0 \quad \text{at} \quad x = 0, a, \\ w = \psi = M_{yy} = 0 \quad \text{at} \quad y = 0, b. \end{aligned} \tag{15}$$

In particular, time harmonic waves are sought and it is assumed that the model is unbounded in x and y directions. To solve the buckling problem, we assume the solution of governing equations with satisfaction of aforementioned boundary condition as

$$\begin{Bmatrix} w \\ \psi \\ \varphi \end{Bmatrix} = \begin{Bmatrix} w^* \sin(\lambda_m x)\sin(\mu_n y) \\ \psi^* \cos(\lambda_m x)\sin(\mu_n y) \\ \varphi^* \sin(\lambda_m x)\cos(\mu_n y) \end{Bmatrix} \mathrm{e}^{\omega t}, \tag{16}$$

where w^*, ψ^*, and φ^* are arbitrary parameters, ω is a complex angular frequency, $\lambda_m = m\pi/a$ and $\mu_n = n\pi/b$. By substituting Eqs. (16) into Eqs. (13) without the effect of external load ($q = 0$), one gets

$$\kappa Gh[\lambda_m \psi^* + \mu_n \varphi^* + (\lambda_m^2 + \mu_n^2) w^*] + [1 + \xi(\lambda_m^2 + \mu_n^2)]P^* = 0, \tag{17a}$$

$$D\left[\left(\lambda_m^2 + \tfrac{1-\nu}{2}\mu_n^2\right)\psi^* + \tfrac{1+\nu}{2}\lambda_m \mu_n \varphi^*\right] + \kappa Gh(\psi^* + \lambda_m w^*) = 0, \tag{17b}$$

$$D\left[\left(\tfrac{1-\nu}{2}\lambda_m^2 + \mu_n^2\right)\varphi^* + \tfrac{1+\nu}{2}\lambda_m \mu_n \psi^*\right] + \kappa Gh(\varphi^* + \mu_n w^*) = 0, \tag{17c}$$

where P^* is given, for uniform buckling load, by

$$P^* = [1 + \xi(\lambda_m^2 + \mu_n^2)][K_1 + K_2(\lambda_m^2 + \mu_n^2) + c_t\omega + S_1\lambda_m^2 + S_2\mu_n^2]w^*. \tag{18}$$

The simplest case, to derive some results which concern with the buckling of rectangular SLGSs, is obtained when the forces S_1 and S_2 are constants throughout the SLGS. Assuming that there is a given ratio between these forces so that $S_x = -\beta_0$ and $S_2 = -\alpha S_1$. The above system of equations is written as

$$([C] - \beta_0[L])\{\Delta\} = \{0\}, \tag{19}$$

where $\{\Delta\} = \{w^*, \psi^*, \varphi^*\}^T$ is the solution vector. The elements of the symmetric matrix $[C]$ are expressed as:

$$\begin{gathered} C_{11} = kGh(\lambda_m^2 + \mu_n^2) + [1 + \xi(\lambda_m^2 + \mu_n^2)][K_1 + K_2(\lambda_m^2 + \mu_n^2) + c_t\omega], \\ C_{12} = kGh\lambda_m, \quad C_{13} = kGh\mu_n, \quad C_{22} = D\left(\lambda_m^2 + \tfrac{1-\nu}{2}\mu_n^2\right) + kGh, \\ C_{23} = D\tfrac{1+\nu}{2}\lambda_m\mu_n, \quad C_{33} = D\left(\tfrac{1-\nu}{2}\lambda_m^2 + \mu_n^2\right) + kGh, \end{gathered} \tag{20}$$

and the elements $L_{ij} = L_{ji}$ of matrix $[L]$ are given by

$$L_{11} = (\lambda_m^2 + \alpha\mu_n^2)[1 + \xi(\lambda_m^2 + \mu_n^2)], \quad L_{12} = L_{13} = L_{22} = L_{23} = L_{33} = 0. \tag{21}$$

Thus, we get the buckling equation by setting the determinant of the matrix $[C] - \beta[L]$ equal to zero. Solving this equation, we shall find that the assumed buckling of the SLGS is possible only for definite values of β_0. The smallest of these values determines the desired critical value.

If the forces S_1 and S_2 are not constants, the problem becomes more involved, since Eq. (19) has in this case variable coefficients, but the general conclusion remains the same. Let, for example (Timoshenko and Gere 1961, Zenkour 2001)

$$S_1 = -\beta_0 \left(1 - c\frac{y}{b}\right), \quad S_2 = 0, \tag{22}$$

where c is a buckling factor. Equation (20) is still the same while the element L_{11} only in Eq. (21) becomes

$$L_{11} = \lambda_m^2\left(1 - \tfrac{1}{2}c\right)[1 + \xi(\lambda_m^2 + \mu_n^2)]. \tag{23}$$

By changing the buckling factor c, we can obtain various particular cases. For example, $c = 0$ corresponds to the case of a uniformly distributed compressive force ($S_1 = -\beta_0,\ S_2 = 0$), and for $c = 2$ we obtain the case of pure bending. All other values give a combination of bending and compression ($c < 2$) or tension ($c > 2$).

4. Numerical results and discussions

It is to be noted that, we get the buckling equation of the SLGSs using local theory of sheets by setting $\xi = 0$ in Eq. (19). Correspondingly, the critical buckling loads of the local graphene are obtained. The buckling loads for the present SLGSs are obtained with and without the inclusion of nonlocal parameter ξ. In what follows we will use the following dimensionless variables

$$\beta = \frac{a^2}{D}\beta_0, \quad \kappa_1 = \frac{a^4 K_1}{D}, \quad \kappa_2 = \frac{a^2 K_2}{D}, \quad \bar{c}_t = \frac{a^4 c_t}{10^3 D}, \quad \eta = \sqrt{\frac{\xi}{a}}, \tag{24}$$

where β is the dimensionless buckling load, κ_1 and κ_2 are the dimensionless foundation parameters, and $\bar{c}_t$ is the dimensionless viscous damping coefficient, and η is the dimensionless nonlocal parameter. First, in order to show the efficiency and accuracy of the present numerical analysis, the current results are compared with some simpler ones. After that, some applications are added for considering the effects of different parameters on the buckling behavior of the SLGS.

4.1 Validation

To the best of the author's knowledge no published literature is available for comparison the buckling of a SLGS embedded in *visco-Pasternak's* medium. In this article, we restrict to investigate the effects of some parameters like nonlocal parameter, aspect ratio, Winkler-Pasternak's foundation, damping coefficient, and mode numbers on the buckling analysis of the SLGSs. However, the present results can be validated by the other published literatures in the buckling analysis of the SLGSs just embedded in an *elastic* medium (Samaei, Abbasion *et al.* 2011, Golmakani and Rezatalab 2015) or without any elastic foundations (Pradhan and Murmu 2009, Ansari and Sahmani 2003, Hosseini-Hashemi, Kermajani *et al*. 2015). In this regard, the simplified result of this paper for a SLGS embedded in Pasternak medium is compared with the work of Samaei, Abbasion *et al.* (2011). Neglecting the viscus damping coefficient and simplifying the expressions tends to the same results as those in Samaei, Abbasion *et al.* (2011). In fact, the plots presented in Samaei, Abbasion *et al.* (2011) are considered as special cases when compared with the present results.

In the first step of validation, the present results for the uniform nonlocal biaxial buckling load β_0 (nN) of an isotropic square graphene sheet are compared with those of molecular dynamic

Table 1 Comparison of critical biaxial buckling load β_0 of nonlocal square SLGSs with those of MD (Ansari and Sahmani, 2013) and of DQM (Golmakani and Rezatalab 2015)

a (nm)	MD (Ansari and Sahmani 2013)	DQM (Golmakani and Rezatalab 2015)	Present			
			$k=\frac{5}{6}$	$k=\frac{3}{4}$	$k=\frac{\pi^2}{12}$	$k=1$
4.990	1.0837	1.0749	1.07103	1.06849	1.07072	1.07485
8.080	0.6536	0.6523	0.65143	0.65083	0.65136	0.65232
10.77	0.4331	0.4356	0.43529	0.43506	0.43526	0.43562
14.65	0.2609	0.2645	0.26436	0.26429	0.26435	0.26447
18.51	0.1714	0.1751	0.17509	0.17506	0.17509	0.17514
22.35	0.1191	0.1239	0.12383	0.12381	0.12383	0.12385
26.22	0.0889	0.0917	0.09167	0.09166	0.09167	0.09168
30.04	0.0691	0.0707	0.07068	0.07068	0.07068	0.07069
33.85	0.0554	0.0561	0.05613	0.05613	0.05613	0.05613
37.81	0.0449	0.0453	0.04526	0.04526	0.04526	0.04527
41.78	0.0372	0.0372	0.03724	0.03724	0.03724	0.03724
45.66	0.0315	0.0313	0.03128	0.03128	0.03128	0.03128

(MD) simulations as reported by Ansari and Sahmani (2013) and with those of differential quadrature method (DQM) as reported by Golmakani and Rezatalab (2015) in Table 1. It is notable that the material properties of SLGS are taken as $E = 1$ TPa and $\nu = 0.16$. Also, the thickness and the nonlocal effect are fixed as $h = 0.34$ nm and $\xi = 1.81$ nm^2. The present theory needs a value of the shear correction factor k. Four commonly used values of the shear correction factor. They are in good agreement with the results of other investigators. The present theory provides more reliable results in the case of $k = 1$ and $k = 5/6$. As indicated in Table 1, it is obvious that β_0 decreases as the dimension of the SLGS increases. In addition, the present results are in good agreement with those of the reported solutions, especially with those of DQM reported by Golmakani and Rezatalab (2015).

For the sake of comparison, we will discuss the effect of nonlocal parameter. For this purpose, the buckling load ratio is defined as β_{NL}/β_L where β_{NL} represents the buckling load calculated using nonlocal theory and β_L represents the buckling load calculated using local theory. In Tables 1 and 2, we are setting $\kappa_1 = \kappa_2 = \bar{c}_t = 0$. The values of Young's modulus $E = 30 \times 10^6$ Pa and Poisson's ratio $\nu = 0.3$ are used to obtain the numerical values. It is found that, the value of $k = 5/6$ is the appropriate one for the shear correction factor.

In the second step of validation, Table 2 represents a comparison of the critical buckling load ratios obtained by the current analytical solution ($\alpha = 1$) and the DQM solutions of Pradhan and Murmu (2009) for a square SLGS with various side lengths and nonlocal parameters ($a/h = 10$). The results presented by Hosseini-Hashemi, Kermajani *et al.* (2015) using higher-order shear deformation theory (HSDT) are also used. An excellent agreement can be found between the present results and the corresponding ones. It is also observed that the present analytical results are the same as those presented by Hosseini-Hashemi, Kermajani *et al.* (2015) using HSDT. They are slightly lower than those of DQM (Pradhan and Murmu 2009) for most cases. The difference between the present analytical solution and DQM increases with an increase in the value of side length or nonlocal parameter. The dimensionless critical buckling load β (nN) is also presented

Table 2 Comparison of dimensionless critical buckling load β and critical buckling load ratio $\beta_{\mathrm{NL}}/\beta_{\mathrm{L}}$ of nonlocal square SLGSs ($h/a = 0.1$)

a	$\sqrt{\xi}$	β	$\beta_{\mathrm{NL}}/\beta_{\mathrm{L}}$		
			Present	Pradhan and Murmu (2009)	Hosseini-Hashemi, Kermajani *et al*. (2015)
5	0.5	15.6051	0.8352	0.835	0.835
	1.0	10.4413	0.5588	0.560	0.559
	1.5	6.7298	0.3602	0.361	0.360
	2.0	4.4935	0.2405	0.242	0.241
10	0.5	17.8067	0.9530	0.954	0.953
	1.0	15.6051	0.8351	0.836	0.835
	1.5	12.9388	0.6925	0.693	0.692
	2.0	10.4413	0.5588	0.560	0.559
25	0.5	18.5390	0.9922	0.993	0.992
	1.0	18.1133	0.9694	0.970	0.969
	1.5	17.4457	0.9337	0.935	0.931
	2.0	16.5896	0.8878	0.889	0.888

Table 3 Critical buckling load β and critical buckling load ratio $\beta_{\mathrm{NL}}/\beta_{\mathrm{L}}$ of nonlocal rectangular SLGSs for various non-dimensional nonlocal parameter $\eta = \sqrt{\xi/a}$

a/b	h/a	η	β ($\beta_{\mathrm{NL}}/\beta_{\mathrm{L}}$)	
			Present	Hosseini-Hashemi, Kermajani *et al*. (2015)
1.0	0.10	0.0	18.6854 (1.000)	18.6861 (1.000)
		0.1	15.6051 (0.835)	15.6057 (0.835)
		0.2	10.4413 (0.559)	10.4408 (0.559)
		0.3	6.7298 (0.360)	6.7200 (0.360)
		0.4	4.4935 (0.241)	4.4937 (0.241)
	0.01	0.0	19.7281 (1.000)	19.7281 (1.000)
		0.1	16.4759 (0.835)	16.4916 (0.835)
		0.2	11.0239 (0.558)	11.0136 (0.559)
		0.3	7.1053 (0.360)	7.1030 (0.360)
		0.4	4.7443 (0.241)	4.7506 (0.241)
0.5	0.10	0.0	11.9169 (1.000)	11.9171 (1.000)
		0.1	10.6082 (0.890)	10.6084 (0.890)
		0.2	7.9793 (0.670)	7.9794 (0.670)
		0.3	5.6470 (0.474)	**6.7289 (0.576)**
		0.4	4.1478 (0.336)	4.0072 (0.336)
	0.01	0.0	12.3327 (1.000)	12.3327 (1.000)
		0.1	10.9782 (0.890)	10.9782 (0.890)
		0.2	8.2577 (0.670)	8.2577 (0.670)
		0.3	5.8439 (0.474)	**7.1052 (0.576)**
		0.4	4.1478 (0.336)	4.1478 (0.336)

in Table 2. It is observed that β increases as the side length increases and the nonlocal parameter $\sqrt{\xi}$ decreases.

In the third step of validation, Table 3 represents a comparison of the dimensionless critical buckling load β (nN) and critical buckling load ratio β_{NL}/β_L obtained by the current analytical solution ($\alpha = 1$) and the Lévy-type solution of Hosseini-Hashemi, Kermajani *et al.* (2015) for a rectangular SLGS. The effects of various values of dimensionless nonlocal parameter ($\eta =$ 0.0, 0.1, 0.2, 0.3, 0.4), aspect ratios ($a/b =$ 0.5, 1.0) and thickness-to-length ratios ($h/a =$ 0.01, 0.10) on the dimensionless buckling loads and buckling load ratios are investigated. The present results are the same as those presented in Hosseini-Hashemi, Kermajani *et al.* (2015). In fact, some typo errors are reported in Hosseini-Hashemi, Kermajani *et al.* (2015) for the case of $\eta = 0.3$ and $a/b = 0.5$. The corrected buckling load and buckling load ratio are given in this table.

4.2 Applications

After verifying the merit and high accuracy of the present analytical solution, the following new results for the buckling analysis of SLGSs can be used as a benchmark for future research studies. In Tables 4 and Figs. 2-9 based on the present analytical closed-form solution, buckling loads have been performed. The results presented here (except otherwise stated) for $\kappa_1 = 10$ nN, $\kappa_2 = 5$ nN, $\xi = 0.1$ nm^2, and $\bar{c}_t = 0.1$ nN. The suitable values of other parameters are fixed as $h = 0.34$ nm and $b = 10$ nm. Also, the complex angular frequency ω is fixed as $\omega = 0.5 + 0.1\,\mathrm{i}$. Different values are given to visco-Pasternak's parameters $\bar{c}_t$, κ_1, and κ_2, and the dimensionless nonlocal parameter η as well as the buckling factor c appeared in Eq. (22). Benchmark results are presented in Table 3 for future comparisons with other investigators. Additional graphical results are plotted in Figs. 2-9. The values of Young's modulus $E = 1$ GPa and Poisson's ratio $\nu = 0.3$ are used to obtain the numerical buckling loads.

Table 4 presents critical buckling load β and critical buckling load ratio β_{NL}/β_L of nonlocal rectangular SLGSs embedded in viscoelastic medium for various dimensionless nonlocal parameter η. Different values of the viscoelastic medium κ_1, κ_2 and $\bar{c}_t$ are taken under consideration. The critical buckling loads of the SLGS are very sensitive to the inclusion of the viscoelastic medium. The critical buckling loads are increasing with the increase of the parameters

Table 4 Dimensionless critical buckling load β and critical buckling load ratio $\beta_{\mathrm{NL}}/\beta_{\mathrm{L}}$ of nonlocal rectangular SLGSs for various non-dimensional nonlocal parameter $\eta = \sqrt{\xi/a}$

$\bar{c}_t$	κ_1	κ_2	β ($\beta_{\mathrm{NL}}/\beta_{\mathrm{L}}$)				
			$\eta = 0$	$\eta = 0.1$	$\eta = 0.2$	$\eta = 0.3$	$\eta = 0.4$
0.0	0	0	12.1392 (1.000)	10.8060 (0.890)	8.1281 (0.670)	5.7522 (0.474)	4.0819 (0.336)
0.1	10	0	17.0026 (1.000)	15.6694 (0.922)	12.9915 (0.765)	10.6156 (0.625)	8.9453 (0.527)
		2	19.0026 (1.000)	17.6694 (0.930)	14.9915 (0.789)	12.6157 (0.665)	10.9453 (0.577)
		5	22.0026 (1.000)	20.6694 (0.939)	17.9915 (0.818)	15.6157 (0.710)	13.9453 (0.634)
		10	27.0026 (1.000)	25.6694 (0.951)	22.9915 (0.852)	20.6157 (0.764)	18.9453 (0.702)
0.2	10	0	21.0554 (1.000)	19.7223 (0.937)	17.0444 (0.811)	14.6685 (0.698)	12.9981 (0.620)
		2	23.0554 (1.000)	21.7223 (0.942)	19.0444 (0.827)	16.6685 (0.724)	14.9981 (0.652)
		5	26.0554 (1.000)	24.7223 (0.949)	22.0444 (0.847)	19.6685 (0.756)	17.9981 (0.692)
		10	31.0554 (1.000)	29.7223 (0.957)	27.0444 (0.871)	24.6685 (0.795)	22.9981 (0.741)
0.5	10	0	33.2140 (1.000)	31.8808 (0.960)	29.2029 (0.881)	26.8271 (0.811)	25.1567 (0.761)
		2	35.2140 (1.000)	33.8808 (0.965)	31.2029 (0.888)	28.8271 (0.821)	27.1567 (0.774)
		5	38.2140 (1.000)	36.8808 (0.966)	34.2029 (0.896)	31.8271 (0.835)	30.1567 (0.791)
		10	43.2140 (1.000)	41.8808 (0.969)	39.2029 (0.908)	36.8271 (0.853)	35.1567 (0.815)

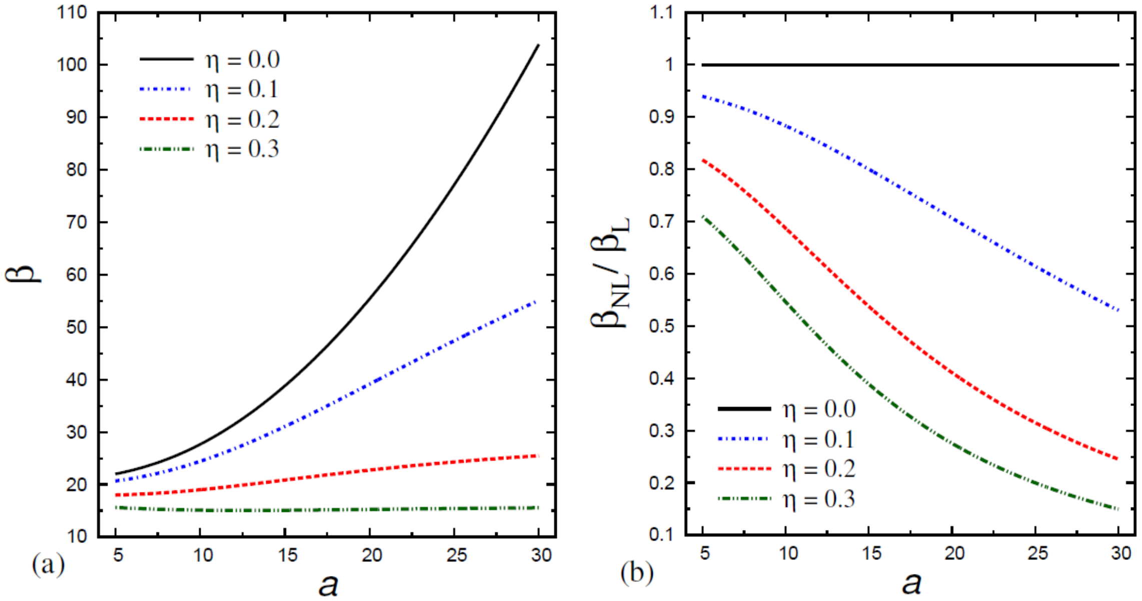

Fig. 2 Critical buckling load β and critical buckling load ratio $\beta_{\mathrm{NL}}/\beta_{\mathrm{L}}$ vs the length a of the SLGS for different nonlocal parameters η

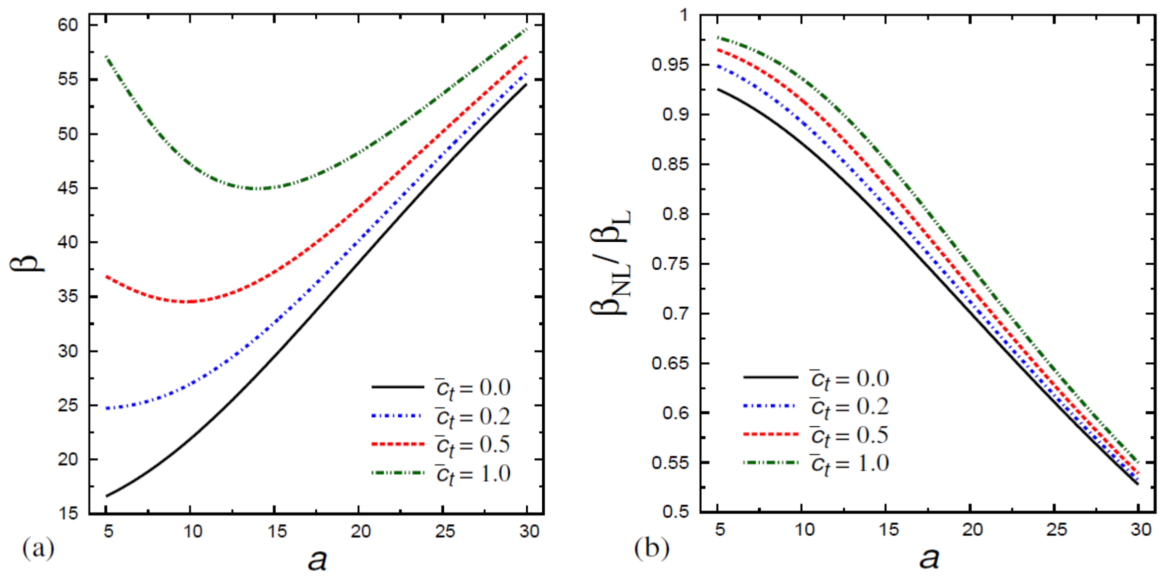

Fig. 3 Critical buckling load β and critical buckling load ratio $\beta_{\mathrm{NL}}/\beta_{\mathrm{L}}$ vs the length a of the SLGS for different damping coefficients $\bar{c}_t$

κ_1, κ_2 and $\bar{c}_t$. In other hand, the buckling loads are decreasing as the dimensionless nonlocal parameter increases. In fact, the largest critical buckling load occurs for higher values of η and without the inclusion of supported viscoelastic medium.

Fig. 2 shows the dimensionless critical buckling load β and critical buckling load ratio

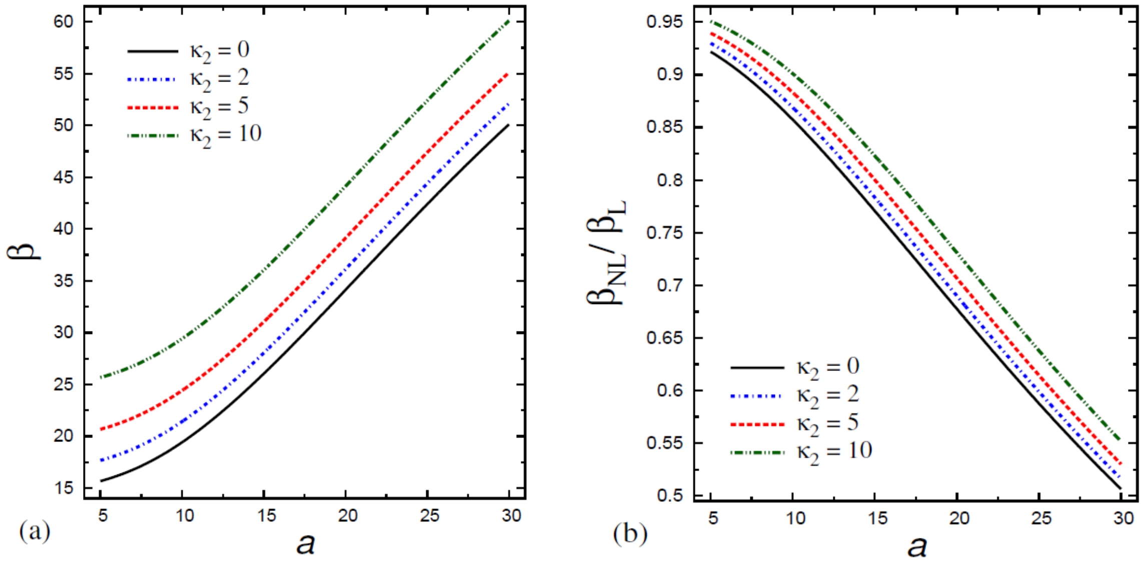

Fig. 4 Critical buckling load β and critical buckling load ratio $\beta_{\mathrm{NL}}/\beta_{\mathrm{L}}$ vs the length a of the SLGS for different Pasternak's parameters κ_2

β_{NL}/β_L versus the variation of the length a of the rectangular SLGS at different nonlocal parameters η. It is observed that local solution for buckling load is greater than the nonlocal ones. This is charged to the effect of small length scale. In addition, increasing the nonlocal parameter decreases the buckling load and the buckling load ratio. This intimates that increasing the nonlocal parameter leads to a decline in stiffness of the SLGS because with decrease of length, the effect of nonlocal parameter reduces.

Fig. 3 shows the dimensionless critical buckling load β and critical buckling load ratio β_{NL}/β_L versus the variation of the length a of the rectangular SLGS for different damping coefficients $\bar{c}_t$. It is observed that nonlocal solutions for buckling load and buckling load ratio with the inclusion of damping coefficients are greater than those for SLGSs embedded in elastic medium only. Increasing the damping coefficient $\bar{c}_t$ increases the buckling load and the buckling load ratio. With increase of length the buckling load ratio β_{NL}/β_L directly decreases. However, the critical buckling load β is increasing as a increases for $\bar{c}_t = 0$ and 0.2. In the case of $\bar{c}_t > 0.2$, β is no longer decreasing and has its minimum for different values of a. In these cases, the maximum buckling load occurs for the smallest and greatest values of the length a.

Fig. 4 presents the critical buckling load β and critical buckling load ratio β_{NL}/β_L versus the variation of the length a of the rectangular SLGS for different Pasternak's parameters κ_2. Once again, the buckling load and buckling load ratio are increasing with the increase of the Pasternak's parameter. With increase of length the critical buckling load β increases while the buckling load ratio β_{NL}/β_L decreases. Fig. 5 shows the dimensionless buckling load β and buckling load ratio β_{NL}/β_L versus the variation of the length a of the rectangular SLGS for different mode numbers m and n. It is interested to note that the critical buckling load β $(m = n = 1)$ is the smallest one while the critical buckling load ratio β_{NL}/β_L is the greatest one.

As the mode numbers increase the buckling load β increases and the buckling load ratio β_{NL}/β_L decreases. In additions, as the length of the SLGS increases the buckling load β

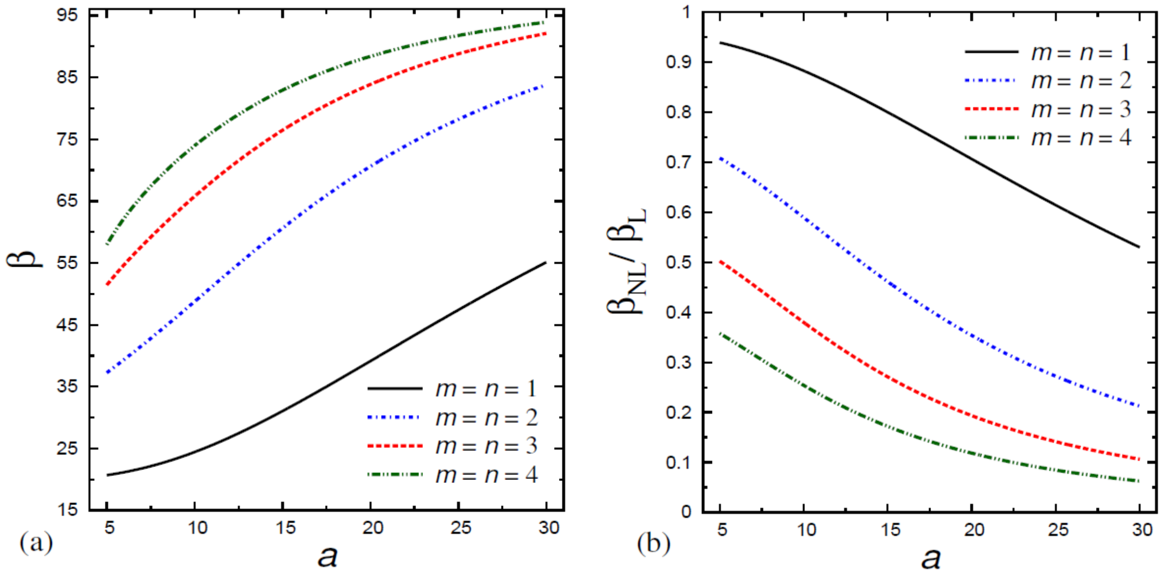

Fig. 5 Buckling load β and buckling load ratio $\beta_{\mathrm{NL}}/\beta_{\mathrm{L}}$ vs the length a of the SLGS for different mode numbers m and n

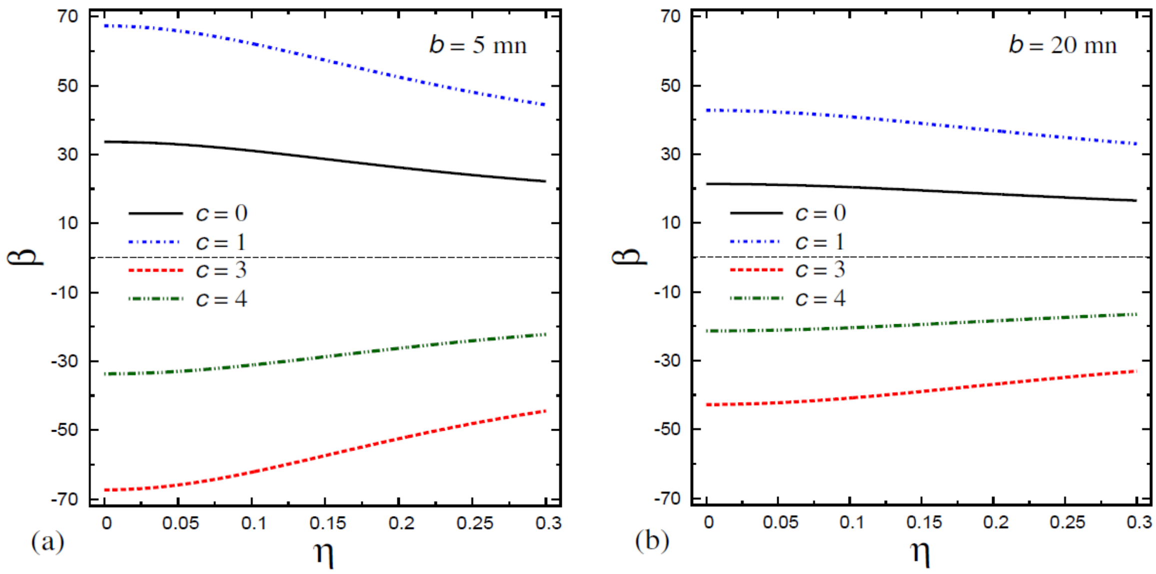

Fig. 6 Nonuniform critical buckling load β vs the nonlocal parameter η of the SLGS for different values of c

increases and the buckling load ratio β_{NL}/β_L decreases.

The effect of buckling factor c on the dimensionless buckling load is investigated in Figs. 6-9. Values of $c < 2$ represent compression buckling loads while values of $c > 2$ represent tension buckling loads. The results presented here for $h = 0.34$ nm, $n = 1$ and $a = 10h$. Two values for the width $b = 5$ nm and $b = 20$ nm are considered. The dimensionless buckling loads are

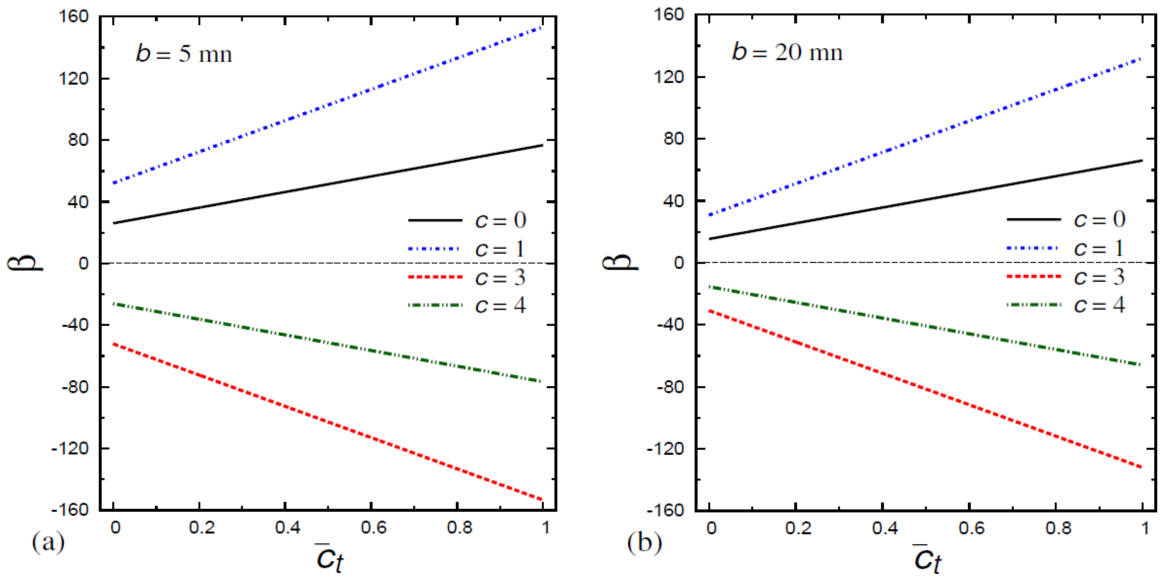

Fig. 7 Nonuniform critical buckling load β vs the damping coefficient $\bar{c}_t$ of the SLGS for different values of c

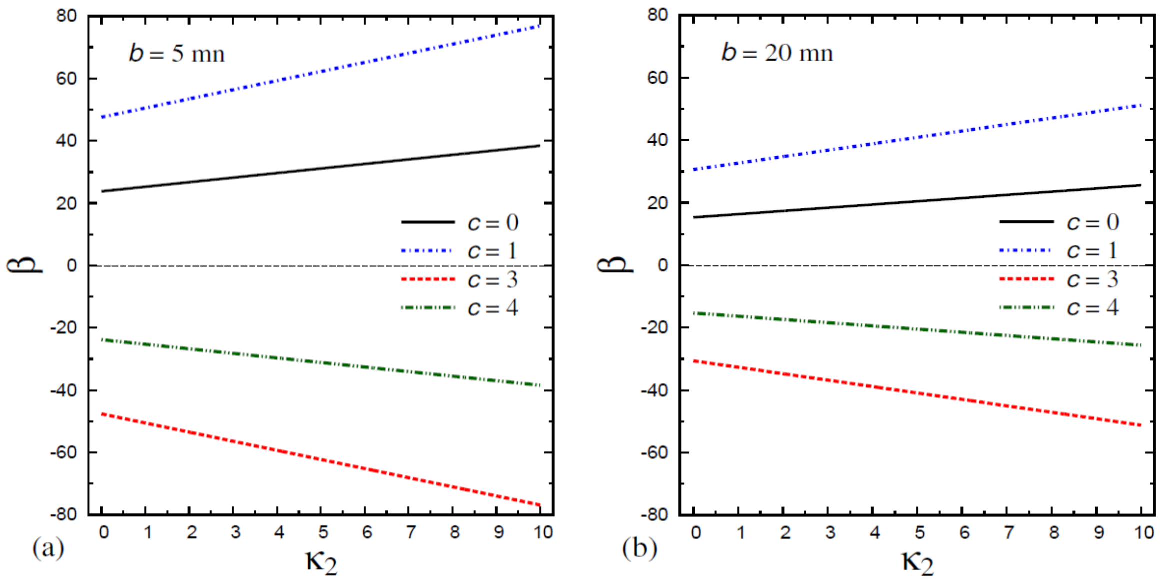

Fig. 8 Nonuniform critical buckling load β vs the Pasternak's parameter κ_2 of the SLGS for different values of c

plotted versus the variation of the nonlocal parameter η, the visco-Pasternak's parameters $\bar{c}_t$ and κ_2, and the mode number m. It is interesting to show that there is a symmetry between the compression buckling loads $(c = 0, 1)$ and the corresponding tension buckling loads $(c = 4, 3)$. Also the magnitudes of the dimensionless buckling loads of the SLGS with $b = 5$ nm are greater than the corresponding ones with $b = 20$ nm. In addition, as c increases the compression

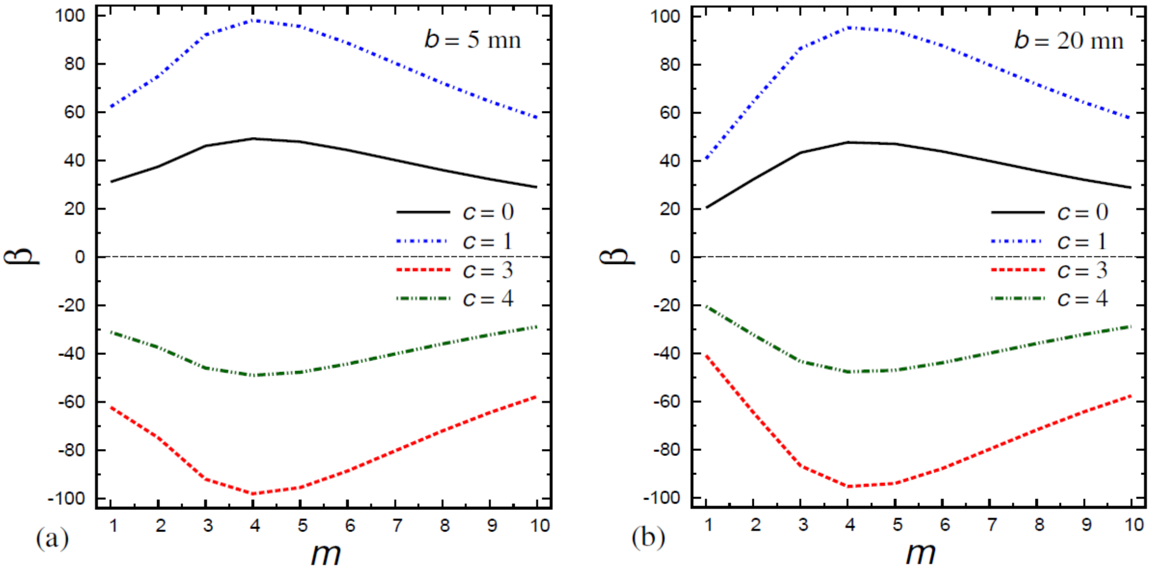

Fig. 9 Nonuniform buckling load β vs the mode number m of the SLGS for different values of c

buckling load increases while tension buckling load decreases. The compression buckling loads are decreasing (the tension buckling loads are increasing) with the increase of the nonlocal parameter η, the visco-Pasternak's parameters $\bar{c}_t$ and κ_2 as shown in Figs. 6-8. However, Fig. 9 shows that absolute value of β is no longer increasing with the variation of the mode number m and has its maximum at $m = 4$.

5. Conclusions

The effect of length scale on uniform and nonuniform buckling behaviors of a single-layer graphene sheet embedded in a visco-Pasternak's elastic medium is investigated using a nonlocal first-order shear deformation plate theory. An explicit solution is extracted for the buckling loads of graphene sheet and the influence of the nonlocal parameter and aspect ratio on dimensionless buckling loads is presented. It is found that the nonlocal assumptions exhibit smaller buckling loads in comparison to the local theory. However, the inclusion of the viscoelastic medium to the graphene sheets exhibits larger buckling loads in comparison to sheets without any viscoelastic medium. The buckling loads are very sensitive to the variation and inclusion of different parameters. It is also concluded that the critical nonuniform buckling load occurs not only at the first mode numbers but also at high values of one of the mode number.

References

Akgöz, B. and Civalek, Ö. (2011), "Strain gradient elasticity and modified couple stress models for buckling analysis of axially loaded micro-scaled beams", *Int. J. Eng. Sci.*, **49**, 1268-1280.

Akgöz, B. and Civalek, Ö. (2012), "Free vibration analysis for single-layered graphene sheets in an elastic

matrix via modified couple stress theory", *Mater. Des.*, **42**, 164-171.
Akgöz, B. and Civalek, Ö. (2013a), "A size-dependent shear deformation beam model based on the strain gradient elasticity theory", *Int. J. Eng. Sci.*, **70**, 1-14.
Akgöz, B. and Civalek, Ö. (2013b), "Buckling analysis of functionally graded microbeams based on the strain gradient theory", *Acta Mech.*, **224**, 2185-2201.
Akgö, B. and Civalek, Ö. (2013c), "Free vibration analysis of axially functionally graded tapered Bernoulli–Euler microbeams based on the modified couple stress theory", *Compos. Struct.*, **98**, 314-322.
Anjomshoa, A., Shahidi, A.R., Hassani B. and Jomehzadeh, E. (2014), "Finite element buckling analysis of multi-layered graphene sheets on elastic substrate based on nonlocal elasticity theory", *Appl. Math. Model.*, **38**, 5934-5955.
Ansari, R. and Sahmani, S. (2013), "Prediction of biaxial buckling behavior of single-layered graphene sheets based on nonlocal plate models and molecular dynamics simulations", *Appl. Math. Model.*, **37**, 7338-7351.
Basua, S. and Bhattacharyya, P. (2012), "Recent developments on graphene and graphene oxide based solid state gas sensors", *Sens. Actuat. B*, **173**, 1-21.
Eringen, A.C. (1983), "On differential equations of nonlocal elasticity, solutions of screw dislocation, surface waves", *J. Appl. Phys.*, **54**, 4703-4710.
Eringen, A.C. (2002), *Nonlocal Continuum Field Theories*, Springer Verlag, New York.
Eringen, A.C. (2006), "Nonlocal continuum mechanics based on distributions", *Int. J. Eng. Sci.*, **44**, 141-147.
Eringen, A.C. and Edelen, D.G.B. (1972), "On nonlocal elasticity", *Int. J. Eng. Sci.*, **10**, 233-248.
Farajpour, A., Solghar, A.A. and Shahidi, A. (2013a), "Postbuckling analysis of multi-layered graphene sheets under non-uniform biaxial compression", *Phys. E*, **47**, 197-206.
Farajpour, A., Dehghany, M. and Shahidi, A.R. (2013b), "Surface and nonlocal effects on the axisymmetric buckling of circular graphene sheets in thermal environment", *Compos B*, **50**, 333-343.
Ghorbanpour Arani, A., Amir, S., Dashti, P. and Yousefi, M. (2014), "Flow-induced vibration of double bonded visco-CNTs under magnetic fields considering surface effect", *Comput. Mater. Sci.*, **86**, 144-154.
Golmakani, M.E. and Rezatalab, J. (2015), "Nonuniform biaxial buckling of orthotropic nanoplates embedded in an elastic medium based on nonlocal Mindlin plate theory", *Compos. Struct.*, **119**, 238-250.
Hosseini-Hashemi, S., Kermajani, M. and Nazemnezhad, R. (2015), "An analytical study on the buckling and free vibration of rectangular nanoplates using nonlocal third-order shear deformation plate theory", *Europ. J. Mech. A/Solids*, **51**, 29-43.
Karličić, D., Cajić, M., Kozić, P. and Pavlović, I. (2015), "Temperature effects on the vibration and stability behavior of multi-layered graphene sheets embedded in an elastic medium", *Compos. Struct.*, **131**, 672-681.
Ke, L.L., Wang, Y.S., Yang, J. and Kitipornchai, S. (2012), "Free vibration of size-dependent Mindlin microplates based on the modified couple stress theory", *J. Sound Vib.*, **331**, 94-106.
Lam, D.C.C., Yang, F., Chong, A.C.M., Wang, J. and Tong, P. (2003), "Experiments and theory in strain gradient elasticity", *J. Mech. Phys. Solid.*, **51**, 1477-1508.
Li, F., Li, J., Feng, Y., Yang, L. and Du, Z. (2011), "Electrochemical behavior of graphene doped carbon paste electrode and its application for sensitive determination of ascorbic acid", *Sens. Actuat. B*, **157**, 110-114.
Lim, C.W., Li, C. and Yu, J.L. (2010), "Dynamic behaviour of axially moving nanobeams based on nonlocal elasticity approach", *Acta Mech. Sinica*, **26**, 755-765.
Mohammadi, M., Farajpour, A., Moradi, A. and Ghayour, M. (2014), "Shear buckling of orthotropic rectangular graphene sheet embedded in an elastic medium in thermal environment", *Compos. B*, **56**, 629-637.
Novoselov, K.S., Geim, A.K., Morozov, S.V., Jiang, D., Zhang, Y., Dubonos, S.V., Grigorieva, I.V. and Firsov, A.A. (2004), "Electric field effect in atomically thin carbon films", *Science*, **306**, 666-669.
Pantelic, R.S., Meyer, J.C., Kaiser, U. and Stahlberg, H. (2012), "The application of graphene as a sample support in transmission electron microscopy", *Solid State Commun.*, **152**, 1375-1382.

Pradhan, S.C. and Murmu, T. (2009), "Small scale effect on the buckling of single-layered graphene sheets under biaxial compression via nonlocal continuum mechanics", *Comput. Mater. Sci.*, **47**, 268-274.

Pradhan, S.C. and Murmu, T. (2010), "Small scale effect on the buckling analysis of single-layered graphene sheet embedded in an elastic medium based on nonlocal plate theory", *Phys. E*, **42**, 1293-1301.

Radić, N., Jeremić, D., Trifković, S. and Milutinović, M. (2014), "Buckling analysis of double-orthotropic nanoplates embedded in Pasternak elastic medium using nonlocal elasticity theory", *Compos. B*, **61**, 162-171.

Reddy, J.N. (2011), "Microstructure-dependent couple stress theories of functionally graded beams", *J. Mech. Phys. Solid.*, **59**, 2382-2399.

Sakhaee-Pour, A. (2009), "Elastic buckling of single-layered graphene sheet", *Comput. Mater. Sci*., **45**, 266-270.

Sakhaee-Pour, A., Ahmadian, M.T. and Vafai, A. (2008), "Applications of single-layered graphene sheets as mass sensors and atomistic dust detectors", *Solid State Commun.*, **145**, 168-172.

Samaei, A.T., Abbasion, S. and Mirsayar, M.M. (2011), "Buckling analysis of a single-layer graphene sheet embedded in an elastic medium based on nonlocal Mindlin plate theory", *Mech. Res. Commun.*, **38**, 481-485.

Timoshenko, S.P. and Gere, J.M. (1961), *Theory of Elastic Stability*, 2nd Edition, McGraw-Hill, New York.

Wang, J., Li, Z., Fan, G., Pan, H., Chen, Z. and Zhang, D. (2012), "Reinforcement with graphene nano-sheets in aluminum matrix composites", *Scripta Mater*., **66**, 594-597.

Xu, Y.M., Shen, H.S. and Zhang, C.L. (2013), "Nonlocal plate model for nonlinear bending of bilayer graphene sheets subjected to transverse loads in thermal environments", *Compos. Struct*., **98**, 294-302.

Yang, F., Chong, A.C.M., Lam, D.C.C. and Tong, P. (2002), "Couple stress based strain gradient theory for elasticity", *Int. J. Solid. Struct.*, **39**, 2731-2743.

Zenkour, A.M. (2001), "Buckling and free vibration of elastic plates using simple and mixed shear deformation theories", *Acta Mech.*, **146**, 183-197.

Zenkour, A.M. (2016a), "Nonlocal transient thermal analysis of a single-layered graphene sheet embedded in viscoelastic medium", *Phys. E*, **79**, 87-97.

Zenkour, A.M. (2016b), "Vibration analysis of a single-layered graphene sheet embedded in visco-Pasternak's medium using nonlocal elasticity theory", *J. Vibroeng.*, **18**, 2319-2330.

Zhang, Y., Zhang, L.W., Liew, K.M. and Yu, J.L. (2016) "Buckling analysis of graphene sheets embedded in an elastic medium based on the kp-Ritz method and non-local elasticity theory", *Eng. Anal. Bound. Elem.* **70**, 31-39.

JL